RESEARCH

Folic acid-functionalized PEGylated niosomes co-encapsulated cisplatin and doxoribicin exhibit enhanced anticancer efficacy

Mona Safari Sharafshadeh[1], Farzaneh Tafvizi[1*], Parvin Khodarahmi[1] and Somayeh Ehtesham[1]

*Correspondence:
farzanehtafvizi54@gmail.com;
Farzaneh.Tafvizi@iau.ac.ir

[1] Department of Biology, Parand Branch, Islamic Azad University, Parand, Iran

Abstract

The medical field is faced with the difficult task of developing a new approach to curing cancer, which is prevalent in organs such as the breast and ovaries and has a high mortality rate. Since chemotherapy is the conventional method of treatment, efforts are being made to improve it to help patients function better. Fortunately, with the use of nanocarriers and their remarkable ability to manage and direct drug delivery, progress is being made in cancer treatment. In addition, folic acid-coated nanocarriers offer several advantages in drug delivery, including improved stability, bioavailability, targeted delivery and drug solubility. These properties make them promising tools for improving cancer treatment efficacy. This research focused on investigating the stability of a specific niosomal formulation (consisting of Span 60 and cholesterol) under different temperature conditions (4 and 25 ℃) for 2 months. In addition, the drug release rate of the formulation was evaluated. The results showed that the size and polydispersity index increased significantly in the stability studies, but the entrapment efficiency% decreased dramatically over time. In addition, encapsulation of drugs in niosomal formulations resulted in stable and slow drug release. The cytotoxicity evaluation results of formulations containing doxorubicin and cisplatin show their significant inhibitory effect on both breast and ovarian cancer cell lines (IC_{50} for DOX–CIS–Nio@PEG–FA formulation was 6.11 and 17.87 μg/mL for A2780 and MCF-7, respectively). Niosomes loaded with a combination of two drugs were found to affect gene expression in the cancer cell lines tested. They decreased the expression of *BCl2, VEGF, CCND1,* and *HER2* genes while increasing the expression of *BAX* gene. Flow cytometry results indicated that niosomes loaded with doxorubicin and cisplatin increased the rate of apoptosis in both cell lines compared to a drug mixture. ROS and cell cycle arrest, confirm the significant inhibition of cancer cells and their destruction in the presence of the synthesized noisome formulation in comparison to free drugs and the combination of two drugs. The potential of this novel approach for delivering drugs to cancer cells lies in the ability to combine treatments and target multiple cancers simultaneously. Such formulations allow co-delivery of drugs to different cancer cells, thereby improving the efficacy of chemotherapy through synergistic effects between drugs.

Graphical Abstract

Introduction

Breast and ovarian cancer are common and recognized cancers that pose a significant risk to women worldwide. Breast and ovarian cancer are common and recognized cancers that pose a significant risk to women worldwide (Smolarz et al. 2022; Akbarzadeh et al. 2022a; Lu et al. 2019). On the other hand, while ovarian cancer has a poor initial 5-year survival rate of 45%, survival tends to stabilize after 10 years of diagnosis (Kim et al. 2022). Extensive research has shown that factors such as breastfeeding, smoking and BMI have a significant impact on long-term survival in these cancers. In addition, chemotherapy is a commonly used treatment strategy; however, it is associated with multidrug resistance and can lead to adverse effects (Nair 2019; Galizia et al. 2018).

Therefore, it is imperative to adopt novel therapeutic strategies that target different mechanisms within cancer cells. However, combination chemotherapy faces several challenges, including drug antagonism, variable drug solubility, and lack of effective tumor cell targeting (Guo et al. 2019; Lovelace et al. 2019). Given the expanding applications of nanotechnology and the need for improved chemotherapeutic approaches, nanoparticles have emerged as a viable solution. Their ability to deliver drugs with precision, mitigate the side effects of chemotherapy, and preserve drug integrity has made them an attractive option (Rizwanullah et al. 2016; Grodzinski et al. 2019; Chen et al. 2019).

The use of nanoparticles in drug delivery systems offers remarkable advantages, including excellent biocompatibility with normal cells and efficient drug uptake by cancer cells (Ayyanaar et al. 2020; Sahrayi et al. 2021). In addition, nanocarriers can be designed to specifically target cancer cell surface proteins, allowing for selective drug delivery and subsequent entry into cancer cells via endocytosis (Akbarzadeh et al. 2020). They can also be used to control drug release and suppress drug-resistant cells. Research has shown that the formulation of nanocarriers with a combination of multiple anticancer drugs leads to more favorable results in terms of anti-tumor effects compared to the delivery of single drugs. This approach utilizes multiple mechanisms simultaneously to effectively eliminate cancer cells (Bhatnagar 2007; Jamshidifar et al. 2021; Hojabri et al. 2023; Navrozoglou et al. 2008).

Most nanoparticles can exhibit cytotoxicity at high concentrations, but the use of niosomal formulations can help overcome this problem (Rostami 2020; Akbarzadeh et al. 2021a). Niosomes are vesicular structures with a mono- or bilayer membrane of non-ionic surfactants and cholesterol, allowing loading of both hydrophilic and hydrophobic drugs (Ghafelehbashi et al. 2019; Naseroleslami et al. 2022). Furthermore, the use of folic acid-coated niosomes has the advantage of targeting cancer cells that overexpress the folate receptor while minimizing damage to normal cells (Rezaei et al. 2022; Sahrayi et al. 2021). Folic acid ligands on the surface of cancer cells can facilitate the selective delivery of drug-loaded niosomes to the tumor site by recognizing and binding to the folate receptors (Aparajay and Dev 2022; Bourbour et al. 2022; Honarvari et al. 2022). In addition, PEGylation of niosomes has the advantage of prolonging the circulation time of the drug in the bloodstream by reducing the clearance by the immune system. As a result, the accumulation of the drug at the site of the tumor is increased (Haroun et al. 2022; Megahed et al. 2022). The acidic pH in the vicinity of cancer cells can induce hydrolysis of surfactant molecules in the structure of the niosomal formulation, allowing drug release in the tumor microenvironment with minimal side effects on normal cells (Akbarzadeh et al. 2020; Rezaei et al. 2022). Numerous experiments, both in vitro and in vivo, have been conducted to evaluate the impact of PEGylated niosomes coated with folic acid on cell toxicity and their efficacy in fighting tumors. These studies have demonstrated the ability of niosomes to inhibit tumor growth, stimulate programmed cell death, and enhance the therapeutic response of anticancer drugs. Synergistic effect of PEGylation, folate targeting and niosome encapsulation maximizes drug accumulation in cancer cells while minimizing exposure to healthy tissue (Rezaei et al. 2022; Sahrayi et al. 2021; Bourbour et al. 2022; Honarvari et al. 2022).

Cisplatin (diaminodichloroplatin) (CIS) is a well-known and highly important drug that is used in the treatment of cancer. It is an inorganic compound that exhibits hydrophobic properties and functions similarly to alkylating agents. The central platinum atom in cisplatin forms covalent bonds with the nitrogen 7 of the guanine and adenine bases in DNA. This binding triggers the activation of proteins that detect cellular damage, leading to the formation of additional compounds within the cell and the initiation of an apoptotic signal (Kanaani et al. 2017; Shen et al. 2012). Cisplatin has demonstrated favorable therapeutic responses in patients undergoing chemotherapy. However, the development of drug resistance, often caused by epigenetic changes at the molecular and cellular levels, leads to disease recurrence (Kanaani et al. 2017).

Doxorubicin (DOX) is another important chemotherapeutic agent used in chemotherapy. It is an antibiotic with hydrophilic properties that allow it to bind to DNA and disrupt the function of topoisomerase II, thereby inhibiting the cell replication process. Despite its widespread use in the treatment of cancer, doxorubicin lacks specificity in terms of cell targeting, which can lead to adverse effects on a wide range of cells (Shafei et al. 2017; Thorn et al. 2011).

Taken together, the research on folic acid-coated PEGylated niosomes underscores their potential to be an exciting drug delivery system for the targeted treatment of cancer. These studies provide insight into the benefits of this approach, such as enhancement of the anti-cancer properties of drugs, improvement of patient outcomes and reduction of side effects associated with conventional chemotherapy.

To address the challenges of chemotherapy, including drug resistance and disease recurrence, nanotechnology has emerged as a breakthrough solution with its targeted approach using nanocarriers. These remarkable nanocarriers interact with the body at the molecular level and have the potential to revolutionize cancer treatment by delivering drugs exclusively to the targeted tissues. In this landmark study, we developed a novel drug combination, doxorubicin and cisplatin, encapsulated in folic acid-coated PEGylated niosomes, representing a major advance in cancer therapy. This innovative nanocarrier design not only allows for a reduction in drug dosage, but also maximizes the therapeutic efficacy of the treatment. By encapsulating both drugs in a single structure, we have achieved a synergistic effect that holds great promise for fighting breast and ovarian cancer simultaneously. Furthermore, our study investigates cytotoxic effects and apoptotic induction on MCF7 and A2780 cancer cells using various advanced methods. With this groundbreaking research, we are paving the way for a new era in cancer treatment by harnessing the power of niosomes to deliver a potent combination of drugs with unparalleled precision. These results set the stage to continue exploring and advancing this innovative strategy in oncology.

Experiments

Materials

Doxorubicin and cisplatin were purchased from BIO BASIC (Markham, ON, Canada). A2780 and MCF-7 cell lines were obtained from Pasteur Cell Bank, Iran. RPMI-1640 medium, DMEM, FBS, PBS, trypsin–EDTA, trypan blue, MTT, and penicillin/streptomycin 100 $\times$ were purchased from Gibco, USA. An annexin V/propidium iodide (PI) assay kit, commonly referred to as an apoptosis detection kit, was provided by Roche (Munich, Germany). The DCFDA/H2DCFDA cellular ROS assay kit was purchased from Thermo Fisher Scientific. Invitrogen (Camarillo, CA, USA) provided the Caspase-3/7 kits. Amicon (Ultra-15 Membrane, MWCO 30000 Da), 1,2-distearoyl-sn-glycero-3-phosphoethanolamine-*N*-[folate(polyethylene glycol)-2000] (ammonium salt) (DSPE–PEG(2000)–Folate), DSPE–PEG (2000), chloroform, ethanol, Span 60, DMSO, Cholesterol, and SDS were purchased from Merck, Germany Dialysis membrane (MWCO 12000 Da). RNA extraction kit was provided by Cinnagen (Iran). RevertAidTM first-strand cDNA synthesis kit from Fermentas (Vilnius, Lithuania) was used for cDNA synthesis.
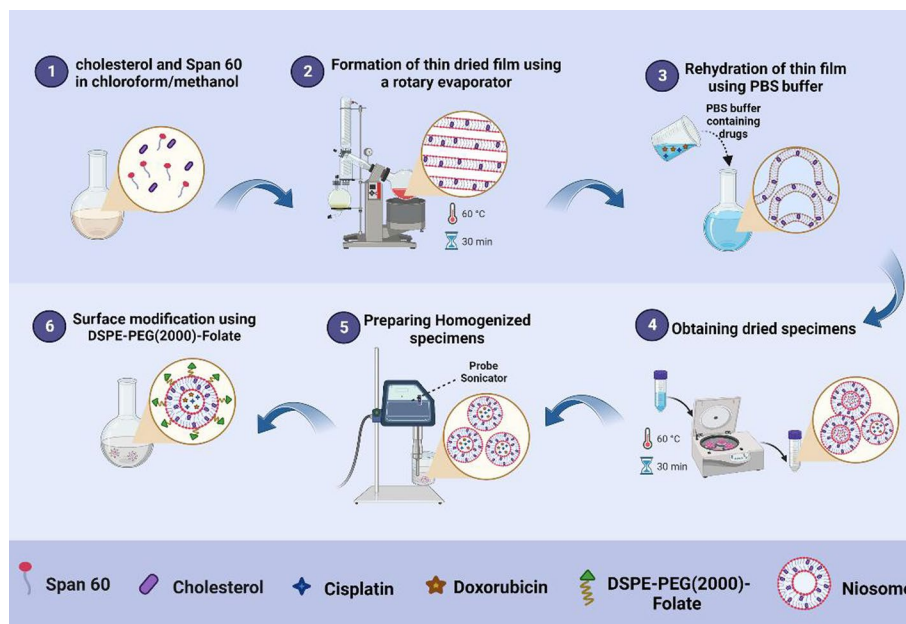
Fig. 1 Preparation of cisplatin and doxorubicin co-encapsulated in a folic acid-decorated PEGylated noisome (DOX–CIS-Nio@PEG–FA)

Optimization of the niosomal formulations

Response surface methodology (RSM) using the Box–Behnken method was used to optimize niosomal formulations. In this study, the effects of lipid, sonication time and molar ratio of surfactant to cholesterol on particle size, polydispersity index (PDI) and entrapment efficiency (EE%) of niosomal formulations were evaluated. Design-Expert software (version 13, Stat-Ease, Inc., Minneapolis, MN, USA) was used to obtain the polynomial equation. The optimized indicator was applied to the Box–Behnken design data. The experimental data were compared with the predicted responses to identify the optimal formulation for further study on the basis of the point prediction method (Sharafshadeh et al. 2023).

Synthesis of PEGylated niosomes coated with folic acid

The synthesis of niosomes coated with PEG–folic acid (DOX–CIS–Nio@PEG–FA) was performed by thin layer hydration method according to previous studies with few modifications. Briefly, the components including span 60, cholesterol and DSPE–PEG (2000)-folate were dissolved in chloroform and evaporated for 30 min using a rotary evaporator (160 rpm, 60 °C). The resulting thin film was then hydrated with PBS containing 10 mg cisplatin and 10 mg doxorubicin (1 ×, 25 °C, 150 rpm, 30 min). To obtain a uniform size distribution, the prepared samples were sonicated for 5 min. Drug loaded niosome formulations were prepared by loading drugs during the synthesis process. Empty niosome constructs without drugs were also synthesized. The schematic synthesis of the DOX–CIS–Nio@PEG–FA is shown in Fig. 1. The optimal formulation was stored at 4 °C for further studies. The levels of surfactant/cholesterol ratio, lipids and sonication time considered are listed in Table 1 (Bourbour et al. 2022; Yeganeh et al. 2022).

Table 1 Desirability criteria and predicted values for the variable, DOX + CIS

Desirability	Lipid—µmoL	Sonication time—min	Surfactant: Cholesterol—molar ratio	Number
0.748	264.7	6.804	1.643	1

Verification of nanoparticle structure

Confirmation of the structure and morphology of the synthesized nanoparticles was performed using various techniques of SEM, TEM, DLS, XRD, DSC and FTIR. The most suitable size and morphology of niosomal nanoparticles were investigated by scanning electron microscopy (SEM) (SSX-500, Shimadzu, Japan) and transmission electron microscopy (TEM) at 80 kV (Netherlands, Philips CM30). Then, the size, particle dispersion index (PDI) and charge of the prepared nanoparticles are checked by dynamic light scattering (DLS) using Malvern Zeta Sizer (Malvern Instruments, UK). X-ray diffraction (XRD) analysis, a non-destructive method that provides comprehensive information on the structure and crystalline phase of materials, was performed on dried synthesized samples on a plane glass (Ni filter and Cu radiation, $\lambda = 0.542$ nm, tube voltage of 25–45 kV and tube current of 100–200 mA). In addition, Fourier Transform Infrared (FT-IR) spectra were used to study chemical bonds, functional groups, and the presence or absence of a bond, using the BRUKER spectrometer (VERTEX 70). Finally, differential scanning calorimetric (DSC) analyses were performed using a differential scanning calorimeter (TA-60, Shimadzu, Japan). Briefly, 3 mg of the samples were sealed in the standard aluminum pans and heated to 300 ℃ at a rate of 5 ℃/min under a purge of nitrogen.

Niosome stability and entrapment efficiency

The stability of optimal niosomes was tested at two temperatures of 4 ℃ and 25 ℃ for 2 months. Subsequently, entrapment efficiency (EE%), size, and polydispersity index (PDI) were evaluated at specific time intervals (Mansoori-Kermani et al. 2022; Targhi et al. 2021).

The encapsulation of drugs (cisplatin and doxorubicin) in nanocarriers was determined by ultrafiltration of the solution containing free drugs and drug-loaded niosomes. The solution was ultrafiltered for 20 min with Amicon Ultra-15 membrane (MWCO 30,000 Da), which resulted in the separation of free drugs (passing through the filter) and drug-loaded niosomes (remaining in the column). Next, the concentration of each drug, cisplatin and doxorubicin, was estimated at the wavelength of the highest absorbance peak (480 nm and 360 nm for doxorubicin and cisplatin, respectively) using UV–Vis spectroscopy (JASCO, V-530, Japan). The concentration of the drugs was calculated based on the standard curve and the provided equation:

$$\text{Encapsulation Efficiency}(\%) = [(A - B)/A] * 100. \tag{1}$$

In this equation, A represents the amount of the primary concentration of cisplatin and doxorubicin for the niosomal preparation, and B defines the amount of the non-entrapped drug after centrifugation (Sharafshadeh et al. 2023).

Release study

The dialysis bag method (MWCO = 12 kDa) was used with an appropriate buffer (50 mL, 1 ×, pH 7.4) to study drug release from the niosome structure. 10 mL of each sample was added to the dialysis membrane. The samples were placed on the stirrer at a speed of 50 rpm and a temperature of 37 ℃. Samples were taken from the external PBS buffer at specified time intervals to determine the rate of drug passage and, finally, to plot the amount of drug released versus time. Different release kinetic models were used to analyze the release profile. The release is determined by the model fitting analysis method (Akbarzadeh et al. 2020).

Cytotoxicity assay

The cytotoxicity of unloaded niosomes, mixed of Doxorubicin/Cisplatin (DOX + CIS), Doxorubicin/Cisplatin-loaded niosomes (DOX + CIS-Nio), and Doxorubicin/Cisplatin-loaded PEGylation niosomes functionalized with folic acid (DOX + CIS–Nio@PEG–FA) was evaluated by calorimetric method using 3-(4,5-dimethylthiazol-2-yl)-2,5-diphenyltetrazolium bromide (MTT) for both MCF7 and A2780 cell lines. Cultured cells were plated (10^4 cells/well) in 96-well plates with RPMI-1640 (containing 1% penicillin–streptomycin and fetal bovine serum) and then incubated for 24 h at 37 °C under a 5% CO_2 atmosphere. Next, defined concentrations (1.25, 2.5, 5, 10, and 20 μg/mL of the samples) were added to the cells and incubated for 48 and 72 h. The medium of each well was then replaced with 0.5 mg/mL MTT. After incubation at 37 °C under 5% CO_2 atmosphere for 4 h, the supernatant was removed and isopropanol was used to dissolve the formed formazan. Finally, the cytotoxicity of the samples was calculated by reading the absorbance of the samples at 570 nm and comparing the absorbance in the treated cells and the control group (untreated cells with the samples) (Sharafshadeh et al. 2023).

ROS assay

The amount of ROS produced in the presence of each sample was checked using the H2DCFDA (2′,7′-dichlorodihydrofluorescein diacetate) kit. Briefly, cancer cell lines (A2780 and MCF7) were treated with samples for 48 h (IC_{50} concentration) and then washed with PBS buffer. They were then incubated with 80 mL of H2DCFDA at 37 °C for 30 min. Finally, the intensity of fluorescence emission was measured using a microplate reader for data quantification (Lalami et al. 2022).

Caspase 3/7 activity

The enzymatic activities of caspase 3/7 were evaluated by enzyme-linked immunosorbent assay (ELISA) according to the manufacturer's guidelines, Roche (Germany). Assays were performed after treatment of A2780 and MCF7 cancer cells with various treatments including control, unloaded niosomes, DOX + CIS, DOX + CIS-Nio, and DOX + CIS-Nio@PEG–FA (Sharafshadeh et al. 2023).

Detection of apoptosis/necrosis

The apoptosis rate of each cell line (MCF7 and A2780) was evaluated by treating cells (1×10^5 cells/well) in the presence of formulations at IC_{50} concentration for 48 h, and

then the cells were examined by Annexin V/Propidium Iodide (PI) assay. Finally, the apoptosis rate of treated cells and untreated cells (control) was compared by flow cytometry (Asghari Lalami et al. 2023).

Profile of gene expression

The expression rate of apoptosis-related genes (*BAX, BCL2, VEGF, CCND1* and *HER2*) was investigated by qRT-PCR method in MCF7 and A2780 cells (Bioneer, Daejeon, South Korea). RNA from treated and untreated cells with samples was isolated using an extraction kit (Qiagen, Germantown, MD), and the concentration of RNAs was measured by photon nanometer (IMPLEN GmbH, Munich, Germany), then complementary DNA was also synthesized using Revert AidTM First Strand cDNA Synthesis Kit (Fermentas, Vilnius, Lithuania). In following, a reaction mixture containing buffer (5 ×, 5 μL), the extracted RNA (1 μg), a random hexamer primer (0.5 μL), the oligo dT primer (0.5 μL), deoxynucleotide triphosphate mixture (10 mM, 2 μL), RNase enzyme inhibitor (20 units/microliter, 1 μL), reverse transcriptase enzyme (1 μL), and double-distilled water (up to a final volume of 20 μL) was prepared. The temperature program was set as follows: 25 °C for 5 min, 42 °C for 60 min, 70 °C for 5 min, and 4 °C for 5 min.

We used the primer sequences from our previous study. The following temperature program was used for the qRT-PCR reaction: 95 °C for 1 min, 95 °C for 15 s, and 60 °C for 1 min. Assuming 100% PCR efficiency, the relative gene expression was calculated using the ΔΔCt method (Mohammadi Shivyari at al. 2022) (IC_{50} concentration is used) (Asl et al. 2022).

Cell cycle analysis

Cell cycle and proliferation stages were determined by assessing the DNA content of the cell and staining with propidium iodide (PI), which can bind to cellular DNA. Briefly, cells (1×10^6 cells/well) cultured in complete medium for 24 h were washed three times with PBS buffer and treated with samples for 48 h. The cells were then fixed with cold 70% ethanol (24 h, room temperature) and stained with 500 μL PI solution (dark, 20 min, room temperature). Finally, they were analyzed by flow cytometry. All experiments were performed with IC_{50} concentration and three replicates (Fatemizadeh et al. 2022).

Statistical analysis

Data from cellular and molecular studies were analyzed using Graphpad Prism version 6.01 software (Graphpad, Inc. La Jolla, CA, 92037, USA). In addition, the comparison between the treatment group and the control group was evaluated using one-way ANOVA and *T* test methods, and the minimum significant level was calculated based on *P* < 0.05.
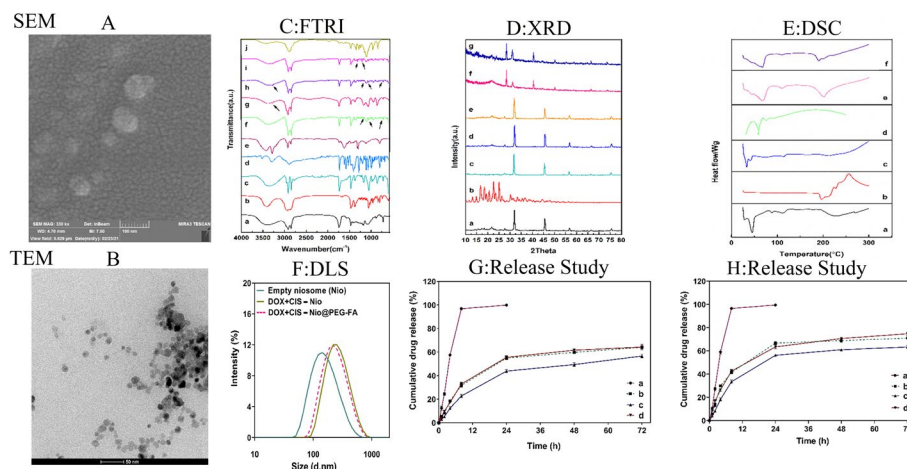
Fig. 2 **A** FE–SEM of DOX–CIS-Nio@PEG–FA, **B** TEM of DOX–CIS-Nio@PEG–FA, **C** FT-IR spectra of different components used for the formation of niosomal formulation, a: span60, b: Cholesterol, c: Niosome, d: DOX, e: CIS, f: DOX-Nio, g: CIS-Nio, h: DOX + CIS-Nio, i: DOX–CIS-Nio@PEG–FA, j: DSPE–PEG2000–PEG–FA, **D** XRD patterns of different samples, a: Niosome, b: DOX, c: CIS, d: DOX-Nio, e: CIS-Nio, f: DOX–CIS-Nio, g: DOX–CIS-Nio@PEG–FA, **E** *Differential Scanning Calorimetry* (*DSC*), a: DOX-Nio, b: DOX, c: Niosome, d: CIS-Nio, e: DOX + CIS-Nio, f: DOX–CIS-Nio@PEG–FA, **F** DLS, **G** In vitro release of CIS, a: free CIS, b: CIS-Nio, c: CIS + DOX-Nio, d: DOX–CIS-Nio@PEG–FA, **H** In vitro release of DOX a: free DOX, b: DOX-Nio, c: DOX + CIS-Nio, and d: DOX–CIS-Nio@PEG–FA

Table 2 Optimized responses obtained by Box–Behnken method and the experimental data for the same responses under the optimum conditions

Parameter	Predicted by Box–Behnken method	DOX–CIS-Nio	DOX–CIS-Nio@PEG–FA	Empty Niosome (Nio)
Average size (nm)	218.73	248.7 ± 7.37	214.6 ± 8.50	143.0 ± 5.47
PDI[a]	0.246	0.214 ± 0.01	0.177 ± 0.009	0.201 ± 0.012
EE[b] (DOX; %)	71.09	80.65 ± 1.80	83.29 ± 1.38	–
EE[b] (CIS; %)	67.27	65.54 ± 1.25	72.73 ± 1.86	–

[a] Polydispersity index

[b] Entrapment Efficiency

Results and discussion

Physicochemical and morphological properties

According to SEM and TEM micrographs, DOX–CIS–Nio@PEG–FA formulation showed spherical and uniform structures (Fig. 2A, B).

Table 2 shows various characteristics of the samples investigated in this study. Considering the minimum particle size, narrow PDI and maximum entrapment efficiency (Table 2), the average size of the optimal samples, empty niosomes (N), doxorubicin/cisplatin-loaded niosomes (DOX + CIS-Nio) and doxorubicin/cisplatin-loaded PEGylation niosomes functionalized with folic acid (DOX–CIS–Nio@PEG–FA) were 143.0 ± 5.47, 248.7 ± 7.37 and 214.6 ± 8.50 nm, respectively. Similarly, the DOX EE% results for DOX + CIS-Nio and DOX–CIS-Nio@PEG–FA were 80.65 ± 1.79 and 83.29 ± 1.38 and the CIS EE% was 65.54 ± 1.25 and 72.73 ± 1.86, respectively. The PDI results show values of 0.201 ± 0.012, 0.214 ± 0.012 and 0.177 ± 0.009 for empty niosomes, DOX + CIS-Nio and DOX–CIS-Nio@PEG–FA, respectively.

Studies report that the size of nanoparticles is directly related to the amount of lipid used in them, so that more lipid leads to larger size. At the same time, the low concentration of cholesterol leads to the compaction of the structure and the reduction of the size of the nanocarriers (Ghafelehbashi et al. 2019; AgSeleci et al. 2016).

PEGylation, the addition of polyethylene glycol (PEG) chains to niosomes, non-ionic surfactant vesicles used for drug delivery, can affect their size. PEGylation can lead to an increase in the size of the niosome due to the formation of a PEG corona, which creates a steric hindrance and hydration around the particles. This swelling can be beneficial for prolonged circulation and increased drug encapsulation capacity. However, in some cases, PEGylation may have minimal effect on niosome size if the PEG chains are short or do not significantly affect the packing arrangement of the niosome components. The specific formulation parameters, including choice of surfactant, lipid composition and PEG chain length, influence the size response. Overall, PEGylation offers advantages, such as improved stability and circulation time, with size changes dependent on formulation factors (Afereydoon et al. 2022; Elliott 2009; Khodabakhsh et al. 2022). The loading of DOX and CIS in the optimal niosome formulation and the functionalization (PEG and FA) of the niosomes lead to an increase in size, based on the data presented in Table 1. Meanwhile, the functionalization is associated with an increase in the encapsulation of both drugs.

The Dox–CIS-Nio@PEG–FA formulation had higher EE% than Dox–CIS-Nio. This result shows that PEGylation of niosomal formulations is important to minimize problems related to niosomal instability, such as drug leakage (Naderinezhad et al. 2017). In addition, polyethylene glycol is hydrophilic and this property renders the surface of the niosomes hydrophilic. As a result, the EE% increased. The results showed that the size of Dox–CIS-Nio@PEG–FA was smaller than Dox–CIS-Nio. A decrease in particle size of Dox–CIS-Nio formulations after PEG modification can be attributed to providing aqueous layer on niosome surfaces by adding PEG (Shehata et al. 2016). This reduction in aggregation would have resulted in the formation of niosomal formulations that were smaller in size than uncoated formulations. These results were supported by other studies in which PEGylation of nanoniosomes improved their stability, increased the entrapment efficiency and reduced the size of the niosomal formulations (Alemi et al. 2018; Moammeri et al. 2022; Haghiralsadat et al. 2017; Hemati et al. 2019; Hemati et al. 2019b).

Figure 2C and Table 3 show the FT-IR spectra for the different components of the niosomal formulation. Part G in the FT-IR diagram shows that when CIS enters the niosome structure, the stretching amine bond has appeared in the 3284 region, which can confirm the proper loading of CIS into the niosome structure. Part F is related to the entry of DOX into the niosome, all the bands related to the niosome were accompanied by a shift to shorter wavelengths, which may be due to the formation of a bond between the DOX and the niosome. In addition, the absorption bands related to the stretching C–O bond of DOX appeared in the 1180 and 1043 regions, which can confirm the successful loading of DOX into the niosome. In addition, the band related to the out-of-plane bending H–O bond appeared in the 780 region, which again can be a reason for the introduction of DOX into the niosome structure. When both drugs enter the niosome structure at the same time (band H), in addition to the DOX bands in the 1178 region, the C–O bond in the 1040 region, and the O–H bond band in

Table 3 Main characteristic peaks for FT-IR spectra of different samples/chemicals

Sample, chemicals	Peak cm^{-1}	Description
Span 60	1125	C–O stretching
	2800–3000	C–H stretching
	3452	OH stretching
Cholesterol	1747	C=O stretching
	2800–3000	C–H stretching
	3452	OH stretching
	1035–1378	CH_2 bending and CH_2 deformation
	1506	C–C stretching in aromatic ring
	1674	C=C stretching
Niosome	1125	C–O stretching
	1747	C=O stretching
	2800–3000	C–H stretching
	3452	OH stretching
Cisplatin	3285	Amin stretching
	1303	Symmetric amine bending
	794	Chlorides stretching
Noisome–cisplatin	3284	Amin stretching
DOX	705–868	Out of plane O–H bending
	1000–1280	C–O stretching of alcohol
	3518	N–H stretching
	1405	CH_3 bending
	1530–1618	Aromatic
	1630	C=O
	1723	Carboxylic acid
	2893	Alkane
	3293	OH
DSPE–PEG2000–folic acid	842	P–O
	961	=C–H out-of-plane bending alkenes
	1060	C–O stretching
	1149 and 1342	C–N stretching
	1242–1281	P=O
	1360	CH_2 It is common in all components
	1468	representing aromatic rings
	1736	C=O Ester
	2889	C=O Aldehyde
	3421	OH

the 778 region, the CIS band also appears in the 3280 region, which is related to the stretching amine bond. All these bonds, while maintaining the niosome structure, may be the reason for the successful loading of both drugs into the niosome at the same time. In addition, when the PEG–folic acid sample was added to the niosomes containing DOX and CIS (lane i), the band related to the C–H bond (PEG) appeared in the 1313 region and the band related to the C–N bond of folic acid appeared in the 1209 region. The changes in the FTIR spectrum can confirm the correct coverage of the niosome containing both drugs simultaneously by DSPE–PEG2000–folic acid (Akbarzadeh et al. 2020; Khodabakhsh et al. 2022).

Figure 2D shows the XRD pattern for the samples tested. Niosome peaks appeared at 21.74, 27.57, 31.88, 45.83, 56.74, 66.63, 75.51° and DOX peaks appeared at 11.67, 12.94, 14.97, 16.75, 18.52, 19.28, 20.55, 22.1, 23.54, 1.36, 1.35 30.19, 31.46, 33.23, 34.25, 35.51, 36.53, 38.30, 39.32, 40.33, 42.36, 44.64° appeared. In addition, when DOX entered the niosome structure, some of the niosome peaks containing DOX became slightly shorter than the niosome and were accompanied by some shift to smaller angles, such that the peaks of the niosome containing DOX appeared at 21.72, 27.51, 31.87, 45.81, 56.72, 66.61, 75.74°, that this change may be due to the presence of the drug in the niosome structure or the reaction of water molecules between the niosome layers. Therefore, since there is no change in the structure of the peaks, it shows that the final formulation has maintained its structure. On the other hand, peaks related to CIS were also formed at 27.32, 31.63, 45.58, 55.49, 66.38 and 75.51°. By adding CIS in the niosome structure, the peaks related to niosome are accompanied by some shift towards smaller angles so that they can be seen at 21.73, 27.55, 31.86, 45.66, 54.03, 56.56, 66.46, 75.59 and the peak 54.03 can be related to CIS drug. Furthermore, by adding both drugs DOX and CIS in the niosome, the peaks related to the niosome were shifted to smaller angles, peaks 21.72, 27.51, 31.30, 40.43, 51.07, 54.78, 66.55, 73.91, it was revealed that the peak 51.07 can be the reason for the presence of CIS in the structure. Finally, the niosome structure containing DOX and CIS was covered by PEG and folic acid, all peaks related to niosome were accompanied by some shift towards smaller degrees of 21.58, 27.43, 30.97, 44.41, 56.32, 66.47, 73.58 and on the other hand with the appearance of peaks at 23.61, 40.61, 46.44, 51.24 in the final formulation can be attributed to the presence of PEG and folic acid as a successful coating of the niosome structure (Bourbour et al. 2022; Lalami et al. 2022).

Differential scanning calorimetry analysis

Differential scanning calorimetry (DSC), a thermal technique that measures the difference in the amount of heat required to raise the temperature of a sample and a reference, is shown in Fig. 2E. For DOX, the observed endothermic points are in the regions of 196.85, 208.89, 227.68, 254.92. With the addition of DOX to niosome, the melting temperature of niosome containing DOX has increased to 33.54, 40.90, 113.65 and 225.88 compared to niosome 33.19, 39.90, 87.89, 113.57, 213.21. According to these findings, DOX can interact with the niosome structure through free hydroxyl functional groups and establish a hydrogen bond, which leads to change the thermal properties of niosome and its higher stability (Afereydoon et al. 2022; Khodabakhsh et al. 2022).

Furthermore, the increase in melting temperature of niosome containing DOX indicates an increase in crystal size and order compared to noisome. On the other hand, the absence of drug melting point in drug-containing niosome is due to the fact that these two compounds have crystallized together and had a good compatibility that they could be encapsulated in the lipid layers of niosome and finally form a new phase (Akbarzadeh et al. 2020; Akbarzadeh et al. 2022b). By adding CIS to niosome, the endothermic points of CIS have melted in the areas of 79, 180, 250, 270 and 280 °C and some niosome structure has been changed due to the formation of hydrogen bond between CIS and niosome. Thus, endothermic points have appeared in the areas of 59.11, 75.20, 91.40 °C, which may be due to the change of thermal properties of niosome and the increase of

its stability. On the other hand, the absence of melting points of CIS in niosome may be due to the appropriate compatibility of drug with niosome and encapsulation of CIS by niosome. Then, by adding both drugs simultaneously in the niosome structure, the melting points of the niosome in the areas of 29.16, 44.38, 68.47, 110.32, 200.36, was accompanied by a decrease in melting point, which could be due to the reaction between the structure of drugs with the niosome and the formation of a new structure, which is associated with a decrease in size. In the final stage, by covering the niosome structure containing two drugs (CIS and DOX) by PEG, FA, endothermic points related to niosome appeared in the areas of 29.16, 44.38, 68.48, 110.33, 19.31, 200.37. The melting point of the drugs did not appear due to the complete encapsulation of the drugs by the lipid layers of niosome and then by PEG and FA, but the melting point of niosome in the mentioned areas was associated due to the formation of bonds with PEG and FA and entering the new phase with slight increase in temperature, which could be the reason for the successful presence of PEG–FA coating and the connection between them with drug-containing niosomes. On the other hand, the melting point of 190.31 °C that appeared in the final formulation may be due to the presence of PEG–FA coating and the formation of a bond between the drug-containing niosomes and the coating.

Drug release

The release profile of CIS and DOX from the dialysis bag containing the combination of two free drugs and drugs co-loaded in niosomes and niosomes functionalized with PEG and folic acid is shown in Fig. 2. The results of the release study show that niosomal formulations control drug release and result in prevention of burst release at physiological condition (pH7.4). As can be seen in Fig. 2G, H, the release of free drugs (both CIS and DOX) quickly reaches its maximum, while the placement of drugs in niosomal structures leads to a controlled and stable release (Rinaldi et al. 2017; Tila et al.

Table 4 Kinetic release models and the parameters obtained for optimum niosomal formulation

Kinetic model	Zero-order		First-order	Higuchi	Korsmeyer–Peppas	
	$C_t = C_0 + K_0 t$		$Log C = Log C0 + K_t / 2.303$	$Q = K_H$	$M_t / M = K_t . t^n$	
	r^2		r^2	r^2	r^2	n^a
DOX (aq)	pH 7.4	0.4530	0.9167	0.6250	0.7474	0.4643
CIS (aq)	pH 7.4	0.4565	0.8475	0.6284	0.7702	0.4543
DOX–CIS-Nio						
DOX	pH 7.4	0.7529	0.8159	0.8967	0.9163	0.6436
CIS	pH 7.4	0.8445	0.8987	0.9532	0.9522	0.6922
DOX–CIS-Nio@PEG–FA						
DOX	pH 7.4	0.7701	0.8694	0.9089	0.9287	0.4951
CIS	pH 7.4	0.8445	0.8987	0.9532	0.9522	0.6922

Zero-order model: where C_t is the drug amount released in time t, C_0 is the initial drug amount in the solution and K_0 is the zero-orderkinetic model constant

First-order model: where C_0 is the initial drug concentration, K_t is the rate constant, and t is the time

Higuchi model: Q is the drug amount released in time t, and K_H is the kinetic model constant

Korsmeyer-Peppa's model: where $M_t / M = K_t . t^n$ is a drug released fraction at time t, n is the release exponent, and K is the release rateconstant

r^2: The regression coefficient

2015). Different models have been used to study the release kinetics. Thus, according to Table 4, the release of free DOX and free CIS at pH7.4 both follow the first-order model, while the release of CIS at the pH 7.4 from co-loaded drugs in niosome structure follows the Higuchi model. However, the Korsmeyer–Peppas model was followed for the release of DOX from the niosome structure containing two drugs at pH 7.4. In addition, the release of DOX and CIS from PEG- and folic acid-functionalized niosomal formulations was investigated for DOX and CIS at pH 7.4, according to the Korsmeyer–Peppas model. The models determined for each of the formulations are based on the r^2 values reported in Table 4; Rinaldi et al. 2017; Tila et al. 2015.
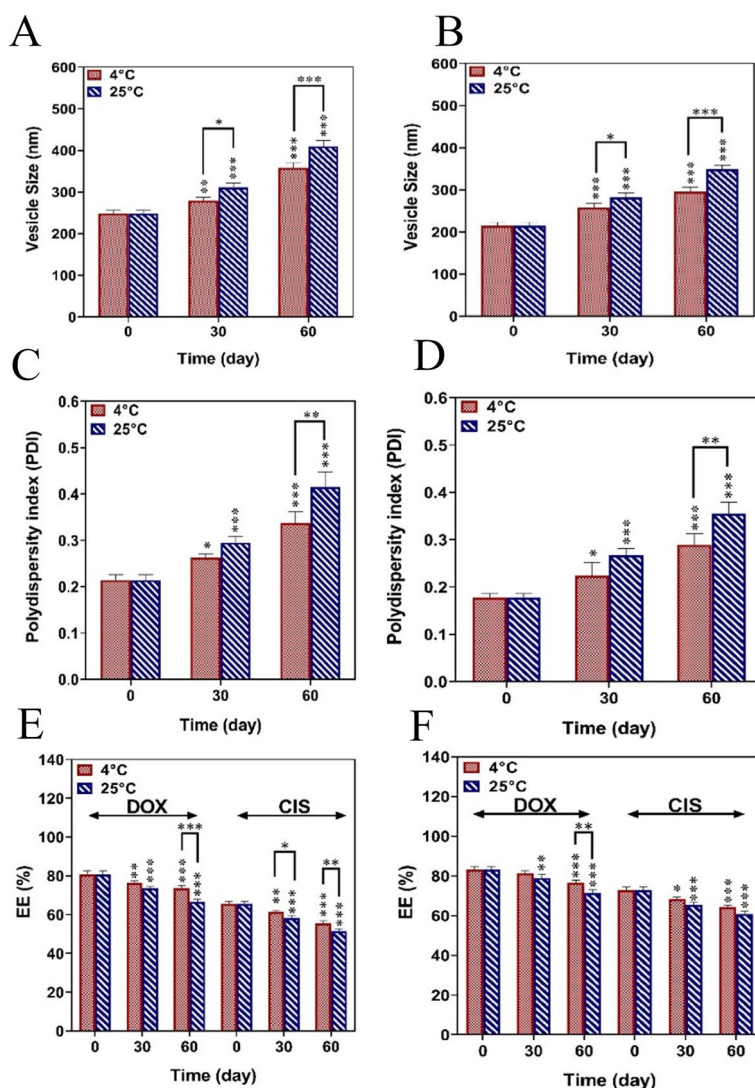
Fig. 3 Effect of storage time and storage temperature on (**A**) average size of DOX + CIS-Nio, (**B**) average size of DOX + CIS-Nio@PEG–FA, (**C**) polydispersity index (PDI) of DOX + CIS-Nio, (**D**) polydispersity index (PDI) of DOX + CIS-Nio@PEG–FA and (**E**) encapsulation efficiency (EE%) of DOX + CIS-Nio, and (**F**) the encapsulation efficiency of DOX + CIS-Nio@PEG–FA. The *P* values are $*P < 0.05$, $**P < 0.01$, $***P < 0.001$

Stability study

Since temperature has a significant effect on the half-life of niosomal structures, to study the stability of the synthesized formulations, the effect of two temperatures (4 ℃ and 25 °C) on the size, PDI and EE% of optimal niosomes (niosomal formulations with CIS and DOX and PEGylated niosomal formulations with both drugs) was evaluated at different time intervals (0, 30 and 60 days). Over time, the size of niosomal vesicles and PDI increased for both temperatures. Meanwhile, the percentage of encapsulation efficiency of two drugs, CIS and DOX, decreased significantly. As a result, the optimal time to store niosome formulations is within a period of 1 month, so that the least changes in size and content occur (Fig. 3). In addition, at a temperature of 4 ℃ compared to 25 ℃, little changes were observed due to the minimal movement of the bilayer in the niosome membrane; therefore, to observe more stability in the niosome structure, the temperature and shorter storage time are of great importance (Chen et al. 2019; Ghafelehbashi et al. 2019; Yinhua et al. 2020).
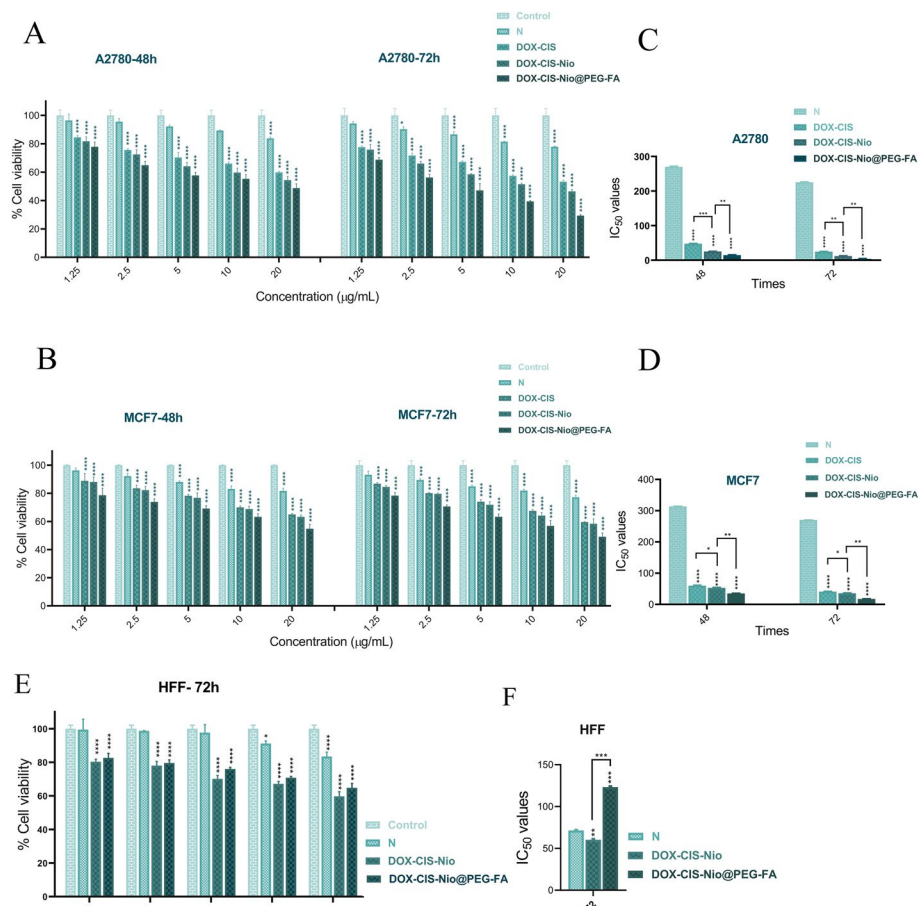
Fig. 4 A In vitro cytotoxic effects of empty niosomes (N), DOX + CIS, DOX + CIS-Nio, and DOX + CIS-Nio@PEG–FA in A2780 cell line; **B** in vitro cytotoxic effects of empty niosomes (N), DOX + CIS, DOX + CIS-Nio, and DOX + CIS-Nio@PEG–FA in MCF-7 cells; **C** comparison between IC_{50} values of all samples in A2780 cells in 48 and 72 h; **D** comparison between IC_{50} values of all samples in MCF7 cells in 48 and 72 h; **E** in vitro cytotoxic effects of empty niosomes (N), DOX + CIS, DOX + CIS-Nio, and DOX + CIS-Nio@PEG–FA in HFF cells; **F** IC_{50} values of all samples in HFF cells in 72 h (Data are represented as mean ± SD and n = 3; ****$P < 0.0001$, ***$P < 0.001$, **$P < 0.01$, *$P < 0.05$). The control sample refers to the cells without treatment

In vitro cytotoxicity analysis

The toxicity effect of designed formulations including empty niosome, combination of CIS and DOX, niosome containing two drugs and FA-PEGylated niosome containing both drugs on A2780 and MCF7 cell lines was evaluated by MTT assay. The effect of the investigated samples on both cell lines was evaluated in two time periods of 48 and 72 h. In addition, a range of concentrations (1.25, 2.5, 5, 10, 20 µg/mL) was used for the calculation of the percentage of cell viability in the presence of our samples. Figures 4A–D shows that the use of different formulations, especially niosomes functionalized with folic acid and PEG (DOX–CIS-Nio@PEG–FA), resulted in a significant decrease in both MCF7 and A2780 cancer cell viability and IC_{50} values. The IC_{50} values of the DOX–CIS-Nio@PEG–FA formulation were determined to be 15.26 and 35.60 µg/mL for the A2780 and MCF-7 cell lines, respectively, after 48 h of exposure. As shown in Fig. 4C, D, IC_{50} of DOX–CIS-Nio@PEG–FA was estimated to be 6.11 and 17.87 µg/mL, respectively, against A2780 and MCF7, respectively, after 72 h of exposure. This indicates a significant decrease compared to DOX–CIS-Nio and DOX–CIS. As expected, the inhibitory effect of the samples on the two cancer cell types increased with increasing concentration and time.

Engineered niosome formulations exhibit enhanced inhibitory effects on cancer cells compared to free drugs. These formulations effectively penetrate the cell membrane and facilitate drug entry into cancer cells. Folic acid, due to its affinity for folate receptors overexpressed on cancer cells, enhances targeted drug delivery to cancer cells, resulting in lower IC_{50} values. This targeted approach increases drug efficacy and reduces toxicity to normal cells. Consequently, nanocarriers containing CIS and DOX are internalized through the interaction between folic acid molecules on the surface of niosome structures and the corresponding receptors on cancer cells (Akbarzadeh et al. 2020; Bourbour et al. 2022). On the other hand, the process of PEGylation, in which polyethylene glycol (PEG) chains are attached to the surface of niosomes, offers numerous advantages. PEGylation increases the stability and durability of niosomes in the bloodstream, resulting in prolonged circulation time and enhanced drug accumulation specifically at the tumor site. This ultimately results in increased therapeutic efficacy and decreased IC_{50} values for cancer cells (Aparajay and Dev 2022; Megahed et al. 2022). The results obtained from the cytotoxicity assay of the samples also support this hypothesisbecause, as shown in Fig. 4A–D, the inhibitory effect of the niosome formulations is much higher compared to the free drug, and niosomes functionalized with PEG and folic acid (DOX–CIS-Nio@PEG–FA) were significantly effective in killing cancer cells and reducing IC_{50} values. According to the results shown in Fig. 4A–D, the combination of CIS and DOX (DOX + CIS) showed an effective synergistic effect compared to the control group. However, the use of nanocarriers containing two drugs played a significant role. According to the results, the observed anti-cancer effect was significant for both cell lines over the duration of the study. However, A2780 cells showed higher sensitivity to treatment compared to MCF7 cells. Overall, the incorporation of folic acid and PEGylation into niosome-based drug delivery systems synergistically improves the targeting ability and the therapeutic efficacy, which leads to lower IC_{50} values for cancer cells. According to the IC_{50} value, DOX–CIS-Nio@PEG–FA showed high biocompatibility towards the healthy HFF cells (Fig. 4E, F). (Wiranowska et al. 2020).
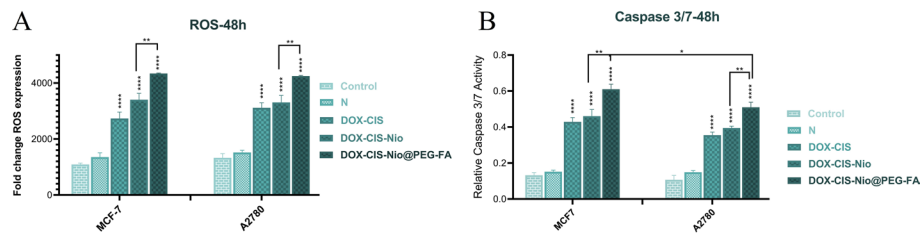
Fig. 5 **A** Caspase 3/7 activity and **B** Changes in intracellular ROS content of MCF7 and A2780 cells treated with different samples. Data represented means ± standard deviations ($n = 3$). For all charts, ****$P < 0.0001$, **$P < 0.01$, *$P < 0.05$

ROS generation and caspase 3/7 activity

Research indicates that a specific level of reactive oxygen species (ROS) promotes cellular growth, whereas an excessive accumulation of ROS in cells leads to cell death (Aggarwal et al. 2019; Cho et al. 2014). Furthermore, oxidative stress plays a crucial role in the development and progression of cancer (Circu and Aw 2010; Ryter et al. 2007). CIS and DOX can promote apoptosis through the generation of ROS to attack the DNA, proteins, and membrane lipids of the cancer cell (Carvalho et al. 2009; Yani et al. 2020; Sadri et al. 2020). In this study, the process of apoptosis in two types of breast and ovarian cancer cells (A2780 and MCF7) with the presence of samples was evaluated by the level of ROS and estimating the oxidation of non-fluorescent DCFH–DA to its elevated fluorescent derivative DCF. Based on the results presented, DOX–CIS, DOX–CIS-Nio, and DOX–CIS-Nio@PEG–FA induced ROS generation in both cell lines compared to control ($P < 0.0001$) (Fig. 5A). However, empty niosomal structures do not induce significant changes in cellular ROS. The designed formulations lead to disruption of mitochondrial function and cell destruction by ROS. Lalami et al. also showed that the activity of ROS was significantly increased in the presence of niosomal nanocarriers on breast cancer cells (Circu and Aw 2010; Ryter et al. 2007).

One of the ways to induce apoptosis is to activate the AKT pathway and alter the regulation of BAX and BCL2, leading to caspase-dependent apoptosis. Caspase-dependent apoptosis, an important form of programmed cell death, is important in the treatment of cancer. This pathway involves the release of cytochrome c from mitochondria, leading to a reduction in mitochondrial membrane potential and subsequent activation of caspase 3/7 (Burz et al. 2009; Fulda and Debatin 2006).

Caspase-3 serves as the primary mediator of apoptotic cell death, taking on the critical role of executing the process. Conversely, caspase-7 plays a supporting role during the execution phase of apoptosis. The results shown in Fig. 5B also indicate that the activity of caspase-3/7 was significantly increased in the presence of DOX–CIS, DOX–CIS-Nio, and DOX–CIS-Nio@PEG–FA ($P < 0.0001$). Caspase-3/7 activity was significantly higher in MCF7 and A2780 cancer cells exposed to DOX–CIS-Nio@PEG–FA compared to DOX–CIS-Nio ($P < 0.01$). Intracellular calcium can be toxic to cells and lead to cell death. DOX–CIS-Nio@PEG–FA niosomal formulations showed higher caspase activity than other samples because increased intracellular calcium leads to increased *BAX* gene expression and decreased *BCL2* gene expression, which
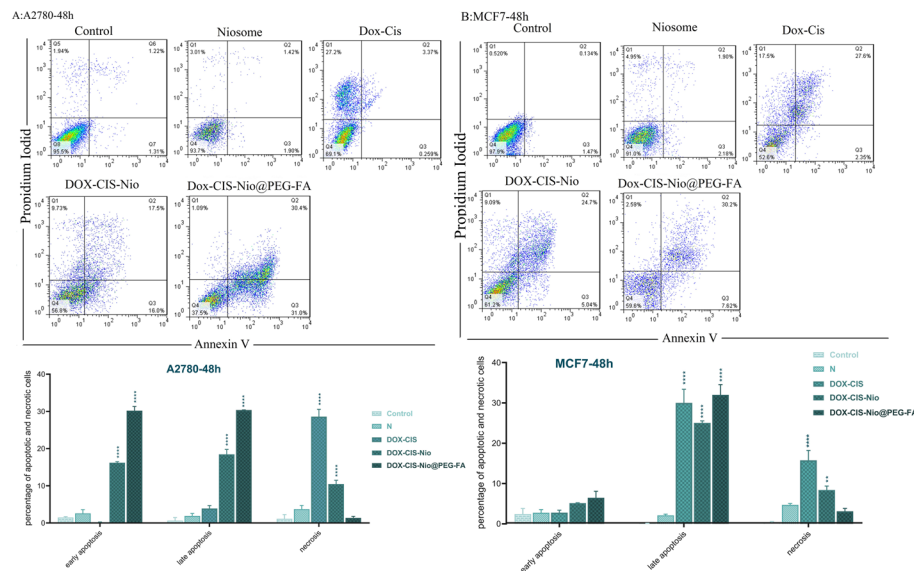
Fig. 6 A Quantitative apoptosis analysis of A2780 cells after treatment with IC_{50} concentration of empty niosomes (N), DOX + CIS, DOX + CIS-Nio, and DOX + CIS-Nio@PEG–FA; **B** quantitative apoptosis analysis of MCF7 cells after treatment with IC_{50} concentration of empty niosomes (N), DOX + CIS, DOX + CIS-Nio, and DOX + CIS-Nio@PEG–FA. The upper left square (Q1) shows the percentage of necrotic cells and the upper right square (Q2) exhibits the percentage of late apoptotic cells, (Q3) exhibits the percentage of early apoptotic cells, and (Q4) shows the percentage of live cells. The data presented means the standard deviation ($n = 3$). For all graphs, ****$P < 0.0001$, **$P < 0.01$. The control sample refers to the cells without treatment

leads to increased caspase expression (Dabbagh Moghaddam et al. 2021; Ho et al. 2016).

Recent reports indicate that the incorporation of drugs into niosomal structures results in a significant increase in caspase 3/7 activity within cancer cells, ultimately leading to apoptosis or programmed cell death (Akbarzadeh et al. 2020; Akbarzadeh et al. 2022b). Furthermore, increased levels of caspase-3 activity are generally considered to be a reliable indicator of apoptosis and serve as a positive marker of cancer treatment efficacy. Recent studies have shown that caspase-3 also plays a role in promoting the growth of cancer cells under stress, as well as facilitating cell migration, invasiveness, and the development of new blood vessels in tumors (Boice and Bouchier-Hayes 2020; Zhou et al. 2018).

Apoptosis/necrosis detection

Apoptosis, a process of cell death, was evaluated in MCF7 and A2780 cancer cells using staining techniques. The investigation aimed to determine the induction of apoptosis in breast and ovarian cancer cells when treated with different samples, including blank niosomes, DOX–CIS, DOX–CIS-Nio, and DOX–CIS-Nio@PEG–FA, all at the IC_{50} concentration. The study focused on exploring how nanocarriers can potentially trigger cancer cell death through the mechanism of apoptosis. The process of identifying apoptotic cells involves the exposure of a specific phospholipid called phosphatidylserine on the cell membrane. This phospholipid can be detected using a sensitive dye called Annexin V. Additionally, dead cells can be distinguished by their interaction with a dye called PI, which binds to DNA but cannot penetrate living cells. Therefore, the amount

of apoptotic activity and the differentiation of healthy, apoptotic and necrotic cells were checked by flow cytometry (Fig. 6A, B). Examination of samples at the early stage of apoptosis in MCF7 and A2780 cells revealed a greater effect on A2780 cells compared to MCF7 cells (i.e., A2780 cells: 16% for DOX–CIS-Nio and 31% for DOX–CIS-Nio@PEG–FA; MCF-7 cells: 5% for DOX–CIS-Nio and 8% for DOX–CIS-Nio@PEG–FA). However, during the late phase of apoptosis, the percentage of apoptotic cells increased significantly for DOX–CIS-Nio and DOX–CIS-Nio@PEG–FA nanoformulations in both cell lines (i.e., A2780 cells: 17% for DOX–CIS-Nio and 30% for DOX–CIS-Nio@PEG–FA; MCF-7 cells: 25% for DOX–CIS-Nio and 30% for DOX–CIS-Nio@PEG–FA). Furthermore, the presence of CIS and DOX combination significantly increased the percentage of cells undergoing necrosis in both A2780 and MCF7 cell lines (27% and 17%, respectively) ($P < 0.0001$). Figure 6A indicates that the presence of DOX–CIS-Nio@PEG–FA resulted in a greater reduction in the percentage of viable cells in the A2780 cells compared to the MCF7 cells. However, both cell lines exhibited a significant increase in the percentage of apoptotic cells when exposed to two designed nanoformulations ($P < 0.0001$): (i.e., MCF-7 cells: 30% for DOX–CIS-Nio and 40% for DOX–CIS-Nio@PEG–FA; A2780 cells: 37% for DOX–CIS-Nio and 60% for DOX–CIS-Nio@PEG–FA). DOX–CIS-Nio@PEG–FA showed the most significant effect in all cases examined based on the results shown in Fig. 6. The data revealed that the DOX–CIS-Nio@PEG–FA formulation significantly enhanced the induction of apoptosis in both A2780 and MCF7 cancer cells compared to the DOX–CIS-Nio formulation ($P < 0.0001$ and $P < 0.01$, respectively).

In summary, doxorubicin and cisplatin have different mechanisms of action. Doxorubicin disrupts DNA replication and transcription processes, while cisplatin forms DNA adducts and causes DNA cross-linking. Both drugs induce DNA damage and activate pathways leading to cell cycle arrest and apoptosis in cancer cells (Abadi et al. 2022; Ji et al. 2022; Nicoletto and Ofner 2022; Song et al. 2022). However, their non-specific targeting can result in adverse effects on healthy cells. While, the folic acid receptors on PEGylated niosomes can facilitate cellular uptake of the nanoparticles by interacting with the receptors on cancer cells. Once internalized, the niosomes can release their payload, such as anticancer drugs or therapeutic agents, directly into the cancer cells, increasing the local concentration of the therapeutic agent at the tumor site. Thus, the use of PEGylated niosomes with folic acid receptors in cancer cell targeting offers several advantages. It improves drug delivery efficiency, reduces systemic toxicity, and enhances the therapeutic efficacy of anticancer agents. Additionally, the ability to actively target cancer cells via folic acid receptors allows for more precise and personalized cancer treatment approaches (Aparajay and Dev 2022; Bourbour et al. 2022; Haroun et al. 2022). In conclusion, the results show that niosomes functionalized with folic acid and PEG played a significant role in inducing apoptosis of the studied cancer cells. The results obtained are consistent with the cytotoxicity results obtained using the MTT assay.

Gene expression analysis

Drugs used to inhibit cancer cells alter the mechanism inside the cell through regulation of gene expression (Joo et al. 2015; Kuwana et al. 2020). The *BAX* gene has a critical function in inducing cell death (apoptosis) by interfering with the mitochondrial
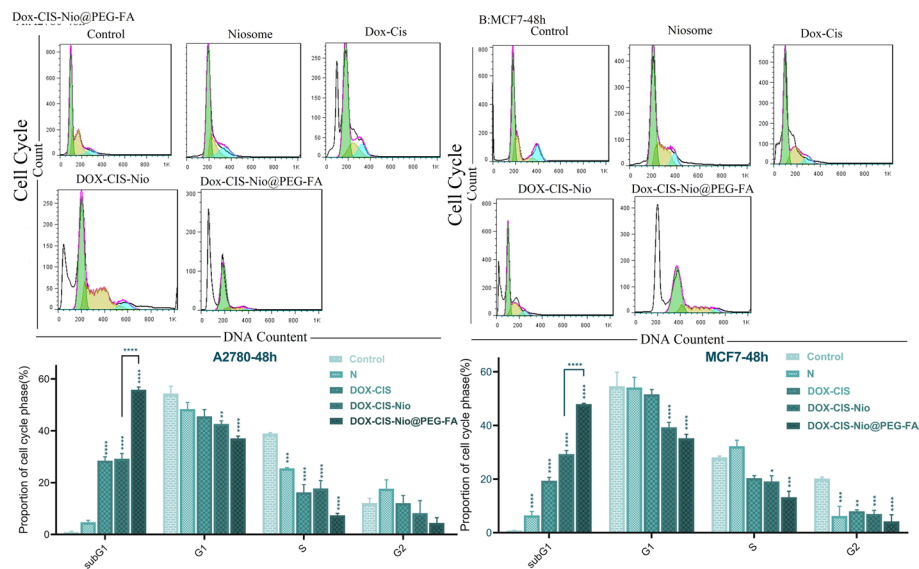
Fig. 7 Comparison of the effect of examined samples on the expression level of *BAX, BCL2, VEGF, CCND1* and *HER2* genes in two cell lines A2780 (**A**) and MCF7 (**B**) cells. Data represent means ± standard deviations (*n* = 3), For all graphs, [****]*P* < 0.0001, [**]*P* < 0.01, [*]*P* < 0.05. The control sample refers to the cells without treatment

membrane. Consequently, the presence of DOX–CIS-Nio and DOX–CIS-Nio@PEG–FA in breast and ovarian cancer cell lines has resulted in a notable increase in the expression of the BAX gene (Fig. 7) (Alam et al. 2022; Lopez et al. 2022). While the *BCL2* gene is an anti-apoptotic gene, the reduction in expression of this gene results in the release of cytochrome c from the mitochondria, which activates caspase genes and induces apoptosis. The results show a decrease in *BCL2* expression in both cell lines, but a significant decrease can be seen in MCF7 (Alam et al. 2022; Zhang et al. 2022). In addition, the *VEGF* gene is associated with cancer and plays a key role in promoting angiogenesis, the formation of new blood vessels. Overexpression of VEGF promotes tumor growth, metastasis, and increased vascular permeability. Targeting VEGF and its signaling pathway is an important therapeutic approach in cancer treatment (Ghalehbandi et al. 2023; Patel et al. 2023). Figure 7 shows that treatment of the cancer cells studied with the samples decreased its expression in both cell lines. HER2 activation also leads to the growth of cancer cells and the activation of anti-apoptotic signals. The human epidermal growth factor receptor 2 (*HER2*) gene plays a critical role in the development of cancer by promoting uncontrolled cell growth and proliferation. In some cancers, particularly breast cancer, the HER2 gene is amplified, resulting in overexpression of the HER2 protein on the cell surface. Overexpression of HER2 leads to increased signaling pathways that promote cell division and survival. This, in turn, contributes to the aggressive growth and progression of HER2-positive cancers. The HER2 protein also plays a role in angiogenesis, invasion, metastasis, and further exacerbating the malignancy of the cancer (Musolino et al. 2022; Damodaran and Olson 2012; Abgarmi, et al. 2021; Swain et al. 2023). Based on the information presented in Fig. 7, the presence of DOX–CIS-Nio and DOX–CIS-Nio@PEG–FA leads to a significant upregulation of the *BAX* gene in both cell lines. However, a downregulation of the *BCL2, VEGF,* and *CCND1* genes was observed
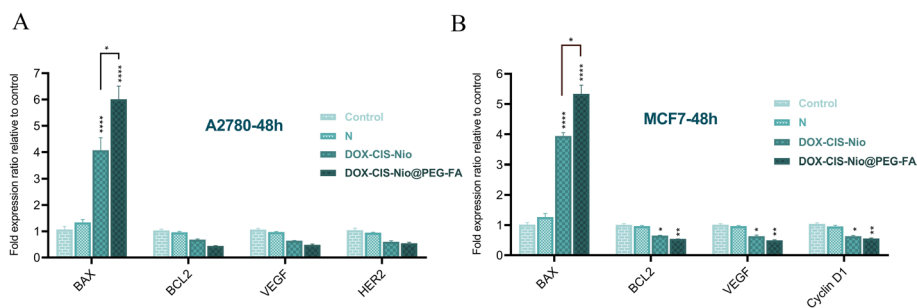
Fig. 8 A Impacts of empty niosomes, DOX + CIS, DOX + CIS-Nio, and DOX + CIS-Nio@PEG–FA on cell cycle arrest after 48 h of treatment on A2780 cancer cells. **B** Impacts of empty niosomes, DOX + CIS, DOX + CIS-Nio, and DOX + CIS-Nio@PEG–FA on cell cycle arrest after 48 h of treatment on MCF7 cells; Data represent means ± standard deviations ($n = 3$), For all graphs, ****$P < 0.0001$, ***$P < 0.001$, **$P < 0.01$, *$P < 0.05$. The control sample refers to the cells without treatment

in MCF7 cells after treatment with two nanoformulations of niosomes. In general, the results presented in Fig. 7 indicate that drugs encapsulated in the structure of niosomes facilitate their uptake into the cell and their effect on gene expression (Circu and Aw 2010; Joo et al. 2015; Kuwana et al. 2020; Pilco-Ferreto and Calaf 2016). Other research studies have also examined the regulation of the genes under investigation and have documented analogous findings (Akbarzadeh et al. 2022a; Ghafelehbashi et al. 2019; Bourbour et al. 2022; Kasravi et al. 2023).

Cell cycle arrest

The effect of treatment of breast and ovarian cancer cells with the samples on their cell cycle progression was investigated by flow cytometry. As shown in Fig. 8A, B, the combined administration of CIS and DOX, CIS–DOX-Nio and DOX–CIS-Nio@PEG–FA resulted in a shift towards the sub-G1 phase of the cell cycle in both breast and ovarian cancer cell lines studied (Fig. 8A, B). This indicates a synergistic effect of the drugs and their enhanced efficacy in inducing cell cycle arrest and potential apoptosis (i.e., MCF7 cells: 19.37% for mixture of CIS and DOX, 29.30% for CIS–DOX-Nio and 48% for DOX–CIS-Nio@PEG–FA; A2780 cells: 28.46% for mixture of CIS and DOX, 29.18% for CIS–DOX-Nio and 55.87% for DOX–CIS-Nio@PEG–FA). These results confirm the increased trend of apoptosis observed in other assays for A2780 and MCF7 cell lines. Furthermore, the studies showed that the percentage of cell cycle arrest varied depending on the specific cancer cell line and the formulation used. The PEGylated niosomes with folate receptors demonstrated higher percentages of cell cycle arrest compared to other formulations, suggesting an enhanced therapeutic effect (Akbarzadeh et al. 2020; Sahrayi et al. 2021; Karimifard et al. 2022). In addition, comparable results regarding the efficacy of drug nanocarriers on the cell cycle of cancer cells have been reported in other studies (Khodabakhsh et al. 2022; Akbarzadeh et al. 2021b).

Conclusion

The most appropriate composition of niosomes, consisting of span 60 and cholesterol, was selected based on size and encapsulation efficiency. To improve their efficiency, the niosomes were modified with PEG and folic acid. Various characteristics of the

Safari Sharafshadeh *et al. Cancer Nanotechnology*   (2024) 15:14

Page 22 of 25

synthesized nanocarriers were then evaluated, including size, composition, interactions, and morphology. The release of both the free drug and the formulated niosomes was measured under pH conditions of 7.4. The toxicity of the synthesized formulations was evaluated along with their effect on the apoptosis rate of breast and ovarian cancer cells. The expression of genes associated with apoptosis was also observed in the treated cell lines. The results confirmed that formulating drugs in niosomes not only allows for controlled drug release, but also facilitates drug penetration into the cells. Furthermore, this approach improves the drug performance and significantly increases apoptosis in the treated cancer cells. The excellent in vitro results encourage us to continue future in vivo studies of CIS and DOX encapsulation in folic acid functionalized PEGylated niosomes.

Declarations

Ethics approval and consent to participate
Not applicable.

Consent for publication
All authors consent to the publication of this study.

Competing interests
The authors report no competing interests.

References
Abadi AJ et al (2022) Curcumin and its derivatives in cancer therapy: potentiating antitumor activity of cisplatin and reducing side effects. Phytother Res 36:189–213
Abgarmi ZM, et al. Breast cancer cell lines, HER2/Neu phenotype, and a higher propensity to reactive oxygen species production. Arch Breast Cancer. 2021;137–142.
Afereydoon S et al (2022) Multifunctional PEGylated niosomal nanoparticle-loaded herbal drugs as a novel nano-radio-sensitizer and stimuli-sensitive nanocarrier for synergistic cancer therapy. Front Bioeng Biotechnol 10:917368
Aggarwal V et al (2019) Role of reactive oxygen species in cancer progression: molecular mechanisms and recent advancements. Biomolecules 9:735
AgSeleci D, Seleci M, Walter JG, Stahl F, Scheper T (2016) Niosomes as nanoparticular drug carriers: fundamentals and recent applications. J Nanomater 2016:1–13
Akbarzadeh I, Yaraki MT, Ahmadi S, Chiani M, Nourouzian DJAPT (2020) Folic acid-functionalized niosomal nanoparticles for selective dual-drug delivery into breast cancer cells: an in-vitro investigation. Adv Powder Technol 31:4064–4071
Akbarzadeh I, Tabarzad M, Khazraei H, Ostovan V (2021a) Development of a novel niosomal formulation for gabapentin. Iran J Colorect Res 9:149–157
Akbarzadeh I et al (2021b) Preparation, optimization and in-vitro evaluation of curcumin-loaded niosome@ calcium alginate nanocarrier as a new approach for breast cancer treatment. Biology 10:173
Akbarzadeh I et al (2022a) The optimized formulation of tamoxifen-loaded niosomes efficiently induced apoptosis and cell cycle arrest in breast cancer cells. AAPS PharmSciTech 23:1–13
Akbarzadeh I et al (2022b) The optimized formulation of tamoxifen-loaded niosomes efficiently induced apoptosis and cell cycle arrest in breast cancer cells. AAPS PharmSciTech 23:57
Alam M et al (2022) Bax/Bcl-2 cascade is regulated by the EGFR pathway: therapeutic targeting of non-small cell lung cancer. Front Oncol 12:933

Alemi A et al (2018) Paclitaxel and curcumin coadministration in novel cationic PEGylated niosomal formulations exhibit enhanced synergistic antitumor efficacy. J Nanobiotechnol 16:1–20

Aparajay P, Dev A (2022) Functionalized niosomes as a smart delivery device in cancer and fungal infection. Eur J Pharm Sci 168:106052

Asghari Lalami Z, Tafvizi F, Naseh V, Salehipour M (2023) Fabrication, optimization, and characterization of pH-responsive PEGylated nanoniosomes containing gingerol for enhanced treatment of breast cancer. Naunyn-Schmiedeberg's Arch Pharmacol 396:6867

Asl SS, Tafvizi F, Noorbazargan H (2022) Biogenic synthesis of gold nanoparticles using Satureja rechingeri Jamzad: a potential anticancer agent against cisplatin-resistant A2780CP ovarian cancer cells. Environ Sci Pollut Res 30:20168

Ayyanaar S et al (2020) ROS-responsive chitosan coated magnetic iron oxide nanoparticles as potential vehicles for targeted drug delivery in cancer therapy. Int J Nanomed 15:3333

Bhatnagar AS (2007) The discovery and mechanism of action of letrozole. Breast Cancer Res Treat 105:7–17

Boice A, Bouchier-Hayes L (2020) Targeting apoptotic caspases in cancer. Biochim Biophys Acta (BBA) Mol Cell Res 1867:118688

Bourbour M et al (2022) Evaluation of anti-cancer and anti-metastatic effects of folate-PEGylated niosomes for co-delivery of letrozole and ascorbic acid on breast cancer cells. Mol Syst Design Eng 7:1102–1118

Burz C, Berindan-Neagoe I, Balacescu O, Irimie A (2009) Apoptosis in cancer: key molecular signaling pathways and therapy targets. Acta Oncol 48:811–821

Carvalho C et al (2009) Doxorubicin: the good, the bad and the ugly effect. Curr Med Chem 16:3267–3285

Chen S, Hanning S, Falconer J, Locke M, Wen J (2019) Recent advances in non-ionic surfactant vesicles (niosomes): fabrication, characterization, pharmaceutical and cosmetic applications. Eur J Pharm Biopharm 144:18–39

Cho SG, Woo SM, Ko SG (2014) Butein suppresses breast cancer growth by reducing a production of intracellular reactive oxygen species. J Exp Clin Cancer Res 33:1–11

Circu ML, Aw TY (2010) Reactive oxygen species, cellular redox systems, and apoptosis. Free Radical Biol Med 48:749–762

Dabbagh Moghaddam F et al (2021) Delivery of melittin-loaded niosomes for breast cancer treatment: an in vitro and in vivo evaluation of anti-cancer effect. Cancer Nanotechnol 12:1–35

Damodaran S, Olson EM (2012) Targeting the human epidermal growth factor receptor 2 pathway in breast cancer. Hosp Pract 40:7–15

Elliott JA. PEGylation of niosomes. 2009.

Fatemizadeh M, Tafvizi F, Shamsi F, Amiri S, Farajzadeh A, Akbarzadeh I (2022) Apoptosis induction, cell cycle arrest and anti-cancer potential of tamoxifen-curcumin loaded niosomes against MCF-7 cancer cells. Iranian J Pathol 17(2):183

Fulda S, Debatin KM (2006) Extrinsic versus intrinsic apoptosis pathways in anticancer chemotherapy. Oncogene 25:4798–4811

Galizia D et al (2018) Self-evaluation of duration of adjuvant chemotherapy side effects in breast cancer patients: a prospective study. Cancer Med 7:4339–4344

Ghafelehbashi R et al (2019) Preparation, physicochemical properties, in vitro evaluation and release behavior of cephalexin-loaded niosomes. Int J Pharm 569:118580

Ghalehbandi S, Yuzugulen J, Pranjol MZI, Pourgholami MH (2023) The role of VEGF in cancer-induced angiogenesis and research progress of drugs targeting VEGF. Eur J Pharmacol 949:175586

Grodzinski P, Moritz K, Michael G, Alberto G (2019) Integrating nanotechnology into cancercare. ACS Nano 13(7):7370–7376

Guo XL et al (2019) Co-delivery of cisplatin and doxorubicin by covalently conjugating with polyamidoamine dendrimer for enhanced synergistic cancer therapy. Acta Biomater 84:367–377

Haghiralsadat F et al (2017) New liposomal doxorubicin nanoformulation for osteosarcoma: drug release kinetic study based on thermo and pH sensitivity. Chem Biol Drug Des 90:368–379

Haroun M et al (2022) Significant of injectable brucine PEGylated niosomes in treatment of MDA cancer cells. J Drug Deliv Sci Technol 71:103322

Hemati M, Haghiralsadat F, Jafary F, Moosavizadeh S, Moradi A (2019) Targeting cell cycle protein in gastric cancer with CDC20siRNA and anticancer drugs (doxorubicin and quercetin) co-loaded cationic PEGylated nanoniosomes. Int J Nanomed 14:6575–6585

Hemati M et al (2019b) Development and characterization of a novel cationic PEGylated niosome-encapsulated forms of doxorubicin, quercetin and siRNA for the treatment of cancer by using combination therapy. Artif Cells Nanomed Biotechnol 47:1295–1311

Ho SS, Murphy KC, Binder BY, Vissers CB, Leach JK (2016) Increased survival and function of mesenchymal stem cell spheroids entrapped in instructive alginate hydrogels. Stem Cell Transl Med 5:773–781

Hojabri M et al (2023) Wet-spinnability and crosslinked fiber properties of alginate/hydroxyethyl cellulose with varied proportion for potential use in tendon tissue engineering. Int J Biol Macromol 240:124492

Honarvari B et al (2022) Folate-targeted curcumin-loaded niosomes for site-specific delivery in breast cancer treatment: In silico and In vitro study. Molecules 27:4634

Jamshidifar E et al (2021) Super magnetic niosomal nanocarrier as a new approach for treatment of breast cancer: a case study on SK-BR-3 and MDA-MB-231 cell lines. Int J Mol Sci 22:7948

Ji P, Wang X, Yin J, Yao Y, Du W (2022) Amplification of ferroptosis with a liposomal nanoreactor cooperates with low-toxicity doxorubicin apoptosis for enhanced tumor chemotherapy. Biomater Sci 10:1544–1553

Joo JH et al (2015) Farnesol activates the intrinsic pathway of apoptosis and the ATF4-ATF3-CHOP cascade of ER stress in human T lymphoblastic leukemia Molt4 cells. Biochem Pharmacol 97:256–268

Kanaani L, Ebrahimifar M, Khiyavi AA, Mehrdiba T (2017) Effects of cisplatin-loaded niosomal nanoparticleson BT-20 human breast carcinoma cells. Asian Pacific J Cancer Prevent APJCP 18:365

Karimifard S et al (2022) pH-responsive chitosan-adorned niosome nanocarriers for co-delivery of drugs for breast cancer therapy. ACS Appl Nano Mater 5:8811–8825

Kasravi M et al (2023) MMP inhibition as a novel strategy for extracellular matrix preservation during whole liver decellularization. Biomater Adv. 156:213710

Khodabakhsh F et al (2022) pH-Responsive PEGylated niosomal nanoparticles as an active-targeting cyclophospha-mide delivery system for gastric cancer therapy. Molecules 27:5418

Kim SJ et al (2022) Epidemiologic risk factors and survival trajectories among epithelial ovarian cancer survivors: a population-based cohort study. Can Res 82:5906–5906

Kuwana T et al (2020) Mitochondrial residence of the apoptosis inducer BAX is more important than BAX oligomeri-zation in promoting membrane permeabilization. J Biol Chem 295:1623–1636

Lalami ZA, Tafvizi F, Naseh V, Salehipour M (2022) Characterization and optimization of co-delivery Farnesol-Gingerol Niosomal formulation to enhance anticancer activities against breast cancer cells. J Drug Deliv Sci Technol 72:103371

Lopez A et al (2022) Co-targeting of BAX and BCL-XL proteins broadly overcomes resistance to apoptosis in cancer. Nat Commun 13:1199

Lovelace DL, McDaniel LR, Golden D (2019) Long-term effects of breast cancer surgery, treatment, and survivor care. J Midwifery Womens Health 64:713–724

Lu HM et al (2019) Association of breast and ovarian cancers with predisposition genes identified by large-scale sequencing. JAMA Oncol 5:51–57

Mansoori-Kermani A et al (2022) Engineered hyaluronic acid-decorated niosomal nanoparticles for controlled and targeted delivery of epirubicin to treat breast cancer. Materials Today Bio 16:100349

Mohammadi Shivyari A, Tafvizi F, Noorbazargan H (2022) Anti-cancer effects of biosynthesized zinc oxide nanoparticles using Artemisia scoparia in Huh-7 liver cancer cells. Inorg Nano-Metal Chem 52(3):375-386

Megahed MA et al (2022) Effect of nanovesicular surface-functionalization via chitosan and/or PEGylation on cyto-toxicity of tamoxifen in induced-breast cancer model. Life Sci 307:120908

Moammeri A et al (2022) pH-responsive, adorned nanoniosomes for codelivery of cisplatin and epirubicin: synergis-tic treatment of breast cancer. ACS Appl Bio Mater 5:675–690

Musolino A et al (2022) Role of Fcγ receptors in HER2-targeted breast cancer therapy. J Immunother Cancer 10:e003171

Naderinezhad S, Amoabediny G, Haghiralsadat F (2017) Co-delivery of hydrophilic and hydrophobic anticancer drugs using biocompatible pH-sensitive lipid-based nano-carriers for multidrug-resistant cancers. RSC Adv 7:30008–30019

Nair PR (2019) Delivering combination chemotherapies and targeting oncogenic pathways via polymeric drug delivery systems. Polymers 11:630

Naseroleslami M et al (2022) Simvastatin-loaded nano-niosomes confer cardioprotection against myocardial ischemia/reperfusion injury. Drug DelivTransl Res 12:1423–1432

Navrozoglou I et al (2008) Breast cancer during pregnancy: a mini-review. Eur J Surg Oncol (EJSO) 34:837–843

Nicoletto RE, Ofner CM III (2022) Cytotoxic mechanisms of doxorubicin at clinically relevant concentrations in breast cancer cells. Cancer Chemother Pharmacol 89:285–311

Patel SA et al (2023) Molecular mechanisms and future implications of VEGF/VEGFR in cancer therapy. Clin Cancer Res 29:30–39

Pilco-Ferreto N, Calaf GM (2016) Influence of doxorubicin on apoptosis and oxidative stress in breast cancer cell lines. Int J Oncol 49:753–762

Rezaei T et al (2022) Folic acid-decorated ph-responsive nanoniosomes with enhanced endocytosis for breast cancer therapy: in vitro studies. Front Pharmacol 13:1101

Rinaldi F et al (2017) pH-sensitive niosomes: effects on cytotoxicity and on inflammation and pain in murine models. J Enzyme Inhib Med Chem 32:538–546

Rizwanullah M, Ahmad J, Amin S (2016) Nanostructured lipid carriers: a novel platform for chemotherapeutics. Curr Drug Deliv 13:4–26

Rostami E (2020) Progresses in targeted drug delivery systems using chitosan nanoparticles in cancer therapy: a mini-review. J Drug Deliv Sci Technol 58:101813

Ryter SW et al (2007) Mechanisms of cell death in oxidative stress. Antioxid Redox Signal 9:49–89

Sadri S et al (2020) Mechanistic computational modeling of the kinetics and regulation of NADPH oxidase 2 assembly and activation facilitating superoxide production. Free Rad Res 54:695–721

Sahrayi H et al (2021) Co-delivery of letrozole and cyclophosphamide via folic acid-decorated nanoniosomes for breast cancer therapy: synergic effect, augmentation of cytotoxicity, and apoptosis gene expression. Pharma-ceuticals 15:6

Sahrayi H et al (2021) Co-delivery of letrozole and cyclophosphamide via folic acid-decorated nanoniosomes for breast cancer therapy: synergic effect, augmentation of cytotoxicity, and apoptosis gene expression. Pharma-ceuticals. 15:6

Shafei A et al (2017) A review on the efficacy and toxicity of different doxorubicin nanoparticles for targeted therapy in metastatic breast cancer. Biomed Pharmacother 95:1209–1218

Sharafshadeh MS, Tafvizi F, Khodarahmi P, Ehtesham S (2023) Preparation and physicochemical properties of cispl-atin and doxorubicin encapsulated by niosome alginate nanocarrier for cancer therapy. Int J Biol Macromol 235:123686

Shehata T, Kimura T, Higaki K, Ogawara KI (2016) In-vivo disposition characteristics of PEG niosome and its interaction with serum proteins. Int J Pharm 512:322–328

Shen DW, Pouliot LM, Hall MD, Gottesman MM (2012) Cisplatin resistance: a cellular self-defense mechanism result-ing from multiple epigenetic and genetic changes. Pharmacol Rev 64:706–721

Smolarz B, Nowak AZ, Romanowicz H (2022) Breast cancer—epidemiology, classification, pathogenesis and treat-ment (review of literature). Cancers 14:2569

Song M, Cui M, Liu K (2022) Therapeutic strategies to overcome cisplatin resistance in ovarian cancer. Eur J Med Chem 232:114205

Swain SM, Shastry M, Hamilton E (2023) Targeting HER2-positive breast cancer: advances and future directions. Nat Rev Drug Discov 22:101–126

Targhi AA et al (2021) Synergistic effect of curcumin-Cu and curcumin-Ag nanoparticle loaded niosome: enhanced antibacterial and anti-biofilm activities. Bioorg Chem 115:105116

Thorn CF et al (2011) Doxorubicin pathways: pharmacodynamics and adverse effects. Pharmacogenet Genomics 21:440

Tila D, Yazdani-Arazi SN, Ghanbarzadeh S, Arami S, Pourmoazzen Z (2015) pH-sensitive, polymer modified, plasma stable niosomes: promising carriers for anti-cancer drugs. EXCLI J 14:21

Wiranowska M et al (2020) Preferential drug delivery to tumor cells than normal cells using a tunable niosome–chitosan double package nanodelivery system: a novel in vitro model. Cancer Nanotechnol 11:1–20

Yani MV, et al. Combination of cisplatin-withaferin based on PEGylated liposome nanoparticles as alternative therapy for ovarian cancer. J Med Health. 2020;2.

Yeganeh FE et al (2022) Formulation and characterization of poly (ethylene glycol)-coated core-shell methionine magnetic nanoparticles as a carrier for naproxen delivery: growth inhibition of cancer cells. Cancers 14:1797

Yinhua D et al (2020) The synthesis, characterization, DNA/BSA/HSA interactions, molecular modeling, antibacterial properties, and in vitro cytotoxic activities of novel parent and niosome nano-encapsulated Ho (III) complexes. RSC Adv 10:22891–22908

Zhang Z et al (2022) Trends in targeting Bcl-2 anti-apoptotic proteins for cancer treatment. Eur J Med Chem 232:114184

Zhou M et al (2018) Caspase-3 regulates the migration, invasion and metastasis of colon cancer cells. Int J Cancer 143:921–930

Publisher's Note